

EMBalance

FP7-ICT-2013-5-2-610454



A Decision Support System incorporating a validated patient-specific, multi-scale Balance Hypermodel towards early diagnostic Evaluation and efficient Management plan formulation of Balance Disorders

PAK – FEM Software

Theoretical Background

1 INTRODUCTION

Finite element method (FEM) divides system in finite number of small elements. Each element is solved with simple set of equations, and then all parts are connected to get solution for large domain. FEM uses variational methods to minimize an error function and produce a stable solution.

A feature of FEM is that it is numerically stable. Errors in the input and intermediate calculations do not accumulate and cause the resulting output to be meaningless. In the first step above, the element equations are simple equations that locally approximate the original complex equations to be studied, where the original equations are often partial differential equations (PDE). The process eliminates all the spatial derivatives from the PDE, thus approximating the PDE locally with

- a set of algebraic equations for steady state problems,
- a set of ordinary differential equations for transient problems.

Many of engineering problems were solved with finite element method.

1.1 PAK - SYSTEM OF PROGRAMS FOR FINITE ELEMENT ANALYSIS

Program PAK is of level of world known packages for structural analysis (graphics, dynamic memory allocation, efficiency, reliability, solution accuracy) and it is built-in finite elements and material models according to the state-of-the art theoretical achievements.

PAK is an open source solver and could be used in various fields for solving partial differential equations, for solving a lot of problems in area of engineering, bioengineering, civil engineering, etc.

Benefits for using PAK:

- Open source architecture written in FORTRAN
- Many publications in the peer review journals, benchmark examples
- Manuals, demos, examples
- Students are using PAK for education
- Developed team from University of Kragujevac and BioIRC with many years of experience
- Parallelization available on different grid platform

1.2 SOLID DYNAMICS

Principle of virtual work

The principle of virtual work is one of the most fundamental principles in mechanics. It is used in many numerical methods as a basis for the development of necessary relations. Here we derive this principle for linear problems: linear material model and small strains.

Formulation of the principle of virtual work

Consider a deformable body in equilibrium, shown in Figure 1, subjected to external loadings and with given boundary conditions. Let assume that a field of virtual displacements δu is imposed, keeping the loading (and stresses) unaltered.

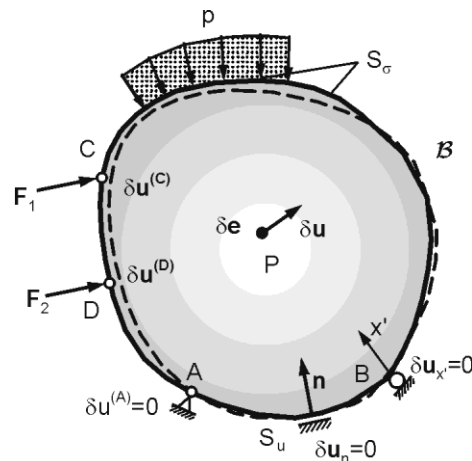


Figure 1: Schematics of deformable body used for the derivation of the principle of virtual work. Virtual displacements and virtual strain at a material point P are δu and δe . Virtual displacements at points of action of forces are $\delta u^{(C)}$ and $\delta u^{(D)}$, while the virtual displacements at the supports are restrained. Virtual displacements correspond to equilibrium state of the body under given loads. Parts of the surface where stresses and displacements are prescribed are S_σ and S_u , respectively.

Those displacements are infinitesimally small and satisfy the displacement boundary conditions. Virtual strains corresponding to the virtual displacements are:

$$\delta e_{ks} = \frac{1}{2} \left[\delta \left(\frac{\partial u_k}{\partial x_s} \right) + \delta \left(\frac{\partial u_s}{\partial x_k} \right) \right] \quad (1)$$

We note here that there are two types of *boundary conditions*: a) stress (loading) and b) displacement boundary conditions. In case a) the stresses can be zero (free surface), or can be given, as in case of

pressure loading shown in Figure 1 Part of the surface where the loading is prescribed is denoted by S_σ . Displacement boundary conditions mean that displacements are prescribed at some points, as the zero displacements at the supports A and B, or for part of the surface, such as $u_n = 0$ shown in the Figure 1. Concentrated forces might act on the body, such as forces F_1 and F_2 shown in Figure 1. It can be proved that in case of a linear elastic material and small displacements, the solution for displacement field within the body is *unique* (uniqueness theorem) for given boundary and loading conditions.

Starting from the equilibrium equations and using the boundary conditions, we finally obtain the following result:

$$\delta W_{\text{int}} = \delta W_{\text{ext}} \quad (2)$$

i.e. the virtual work of internal forces δW_{int} and virtual work of external forces δW_{ext} are equal. The internal and external virtual works are:

$$\delta W_{\text{int}} = \int_V \sigma_{ij} \delta e_{ij} dV = \int_V \delta \mathbf{e}^T \boldsymbol{\sigma} dV \quad (3)$$

and

$$\delta W_{\text{ext}} = \int_V F_k^V \delta u_k dV + \int_{S^\sigma} f_k^S \delta u_k^S dV + \sum_i F_k^{(i)} \delta u_k^{(i)}; \quad \text{sum on } k, \quad k = 1, 2, 3 \quad (4)$$

Here f_k^S and δu_k^S are the distributed surface forces and virtual displacements at the surface is S^σ . Also, $F_k^{(i)}$ and $\delta u_k^{(i)}$ are the components of the concentrated force 'f' and virtual displacement of the material point where this force is acting on the body. Note that the matrix form of virtual work in Equation (3) assumes the stress and strain vectors.

Stiffness Matrix and Nodal Forces.

The internal virtual work can be expressed as:

$$\delta W^{\text{int}} = \int_V \delta \mathbf{e}^T \boldsymbol{\sigma} dV = \delta \mathbf{U}^T \int_V \mathbf{B}^T \mathbf{C} \mathbf{B} dV \mathbf{U} = \delta \mathbf{U}^T \mathbf{K} \mathbf{U} \quad (5)$$

where we have employed the relation $\delta \mathbf{e}^T = \delta \mathbf{U}^T \mathbf{B}^T$, and the constitutive relationship $\boldsymbol{\sigma} = \mathbf{C} \mathbf{e}$. Clearly, the *stiffness matrix* \mathbf{K} is

$$\mathbf{K} = \int_V \mathbf{B}^T \mathbf{C} \mathbf{B} dV \quad (6)$$

The stiffness matrix is symmetric and has dimensions $3N \times 3N$ (in our case 24×24) and the force vector F^{int} is of size $3N$, $F^{\text{int}}(F_x^{(\text{int})1}, F_y^{(\text{int})1}, F_z^{(\text{int})1}, \dots, F_x^{(\text{int})N}, F_y^{(\text{int})N}, F_z^{(\text{int})N})$.

In the case when body forces are present, the corresponding nodal forces are calculated from the equality of virtual work:

$$\int_V \delta \mathbf{u}^T \mathbf{f}^V dV = \delta \mathbf{U}^T \int_V \mathbf{N}^T \mathbf{f}^V dV = \delta \mathbf{U}^T \mathbf{F}^V \Rightarrow \mathbf{F}^V = \int_V \mathbf{N}^T \mathbf{f}^V dV \quad (7)$$

where f^V is the force per unit volume, and F^V is the vector of equivalent volumetric nodal forces. Here, the displacement interpolation has been used.

The external nodal forces resulting from the pressure on an element surface are calculated by employing again the equivalence of virtual work. A simple approximation for the 8-node element is to calculate the total force as $F_p = pA$ (where p as the mean pressure and A is the area of the element side) and use $F_p / 4$ at each node in the mean normal surface direction.

Calculation of the above volumetric integrals must be performed numerically.

Differential equations of motion

Consider a material body subjected to external time dependent forces $F_1(t), F_2(t), \dots$ producing motion and deformation, as schematically shown in Figure 2.

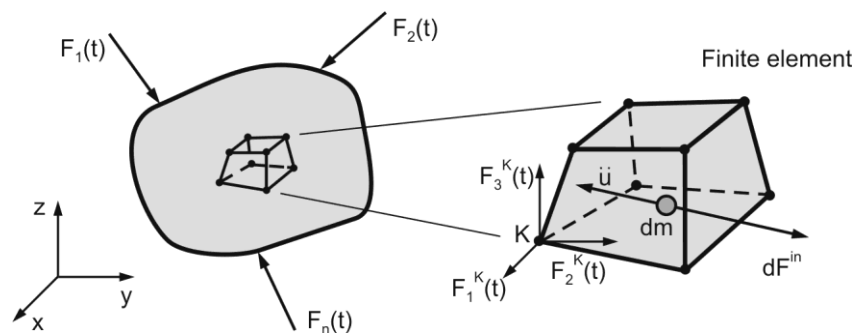


Figure 2: A schematic representation of dynamics of a deformable body. Elementary mass dm within the finite element; elementary inertial force dF^{in} and the time variable nodal force components at a node K.

The motion is such that we must take into account inertial forces. The inertial force dF^{int} of a mass dm is

$$d\mathbf{F}^{in} = -\ddot{\mathbf{u}}dm = -\rho\ddot{\mathbf{u}}dV \quad (8)$$

Where $\ddot{\mathbf{u}} \equiv d^2\mathbf{u}/dt^2$ is the acceleration, ρ is material density, and dV is the elementary volume. The inertial force is a volumetric force and the equivalent nodal inertial force vector \mathbf{F}^{in} follows from Equation (7):

$$\mathbf{F}^{in} = -\int_V \rho \mathbf{N}^T \ddot{\mathbf{u}} dV = -\int_V \rho \mathbf{N}^T \mathbf{N} dV \ddot{\mathbf{U}} = -\mathbf{M} \ddot{\mathbf{U}} \quad (9)$$

Where \mathbf{M} is the element *mass matrix*:

$$\mathbf{M} = \int_V \rho \mathbf{N}^T \mathbf{N} dV \quad (10)$$

And $\ddot{\mathbf{U}}$ is the *nodal acceleration* vector. In derivation of Equation (10) the relationship $\ddot{\mathbf{u}} = \mathbf{N} \ddot{\mathbf{U}}$ is used, which follows from the interpolation of displacements within the finite element. Note that the mass matrix is symmetric, with dimension $3N \times 3N$ for a 3D finite element.

The derived mass matrix is called the *consistent mass matrix*. In practical applications of dynamic FE analysis, a simplified, so-called *lumped mass* matrix is used. The lumped mass matrix is a diagonal matrix with the non-zero terms equal to the element mass divided by the number of element nodes.

When damping (viscous) effects are present within the material, the elementary damping force can be expressed as:

$$d\mathbf{F}^w = -b\dot{\mathbf{u}}dV \quad (11)$$

Where b is the damping (viscous) coefficient. Then, following the above derivation for the element inertial nodal force vector, we obtain the element nodal damping vector \mathbf{F}^w as:

$$\mathbf{F}^w = -\mathbf{B}^w \dot{\mathbf{U}} \quad (12)$$

where \mathbf{B}^w is the element damping matrix:

$$\mathbf{B}^w = \int_V b \mathbf{N}^T \mathbf{N} dV \quad (13)$$

We now substitute the inertial and damping nodal force vectors Equation (9) and Equation (12) into the element equilibrium equation, and further assemble the equilibrium equations to obtain:

$$\mathbf{M}_{sys} \ddot{\mathbf{U}}_{sys} + \mathbf{B}_{sys}^w \dot{\mathbf{U}}_{sys} + \mathbf{K}_{sys} \mathbf{U}_{sys} = \mathbf{F}_{sys}^{ext} \quad (14)$$

where M_{sys} , B_{sys}^w and K_{sys} are the mass, damping and stiffness matrices of the system, respectively; and F_{sys}^{ext} is the system external force vector that includes the external concentrated, surface and body forces. Equation (14) represents the differential equation of motion of a material system discretized into finite elements.

1.3 FLUID DYNAMIC

Navier-Stokes equation was used for 3D viscous fluid inside the chambers (balance of linear momentum, Equation (15)) together with incompressibility condition (Equation (16))

$$\rho \left(\frac{\partial v_i}{\partial t} + v_j \frac{\partial v_i}{\partial x_j} \right) = - \frac{\partial p}{\partial x_i} + \mu \left(\frac{\partial^2 v_i}{\partial x_j \partial x_j} + \frac{\partial^2 v_j}{\partial x_j \partial x_i} \right) \quad (15)$$

$$\frac{\partial v_i}{\partial x_i} = 0 \quad (16)$$

In these equations v_i is the fluid velocity in directions x_i , ρ is the fluid density, p is pressure, μ is the dynamic viscosity; and summation is assumed on the repeated (dummy) indices, $i, j = 1, 2, 3$.

Code was validated using the analytical solution for shear stress and velocities through curve tube. For calculation was used “penalty” formulation.

Incremental – iterative scheme used in PAK solver for the certain time step and equilibrium iteration is show in the equations bellow:

$$\begin{bmatrix} \frac{1}{\Delta t} \mathbf{M}_v + {}^{t+\Delta t} \mathbf{K}_{vv}^{i-1} + {}^{t+\Delta t} \mathbf{K}_{\mu v}^{i-1} + {}^{t+\Delta t} \mathbf{J}_{vv}^{i-1} & \mathbf{K}_{vp} \\ \mathbf{K}_{vp}^T & \mathbf{0} \end{bmatrix} \begin{Bmatrix} \Delta \mathbf{v}^i \\ \Delta \mathbf{p}^i \end{Bmatrix} = \begin{Bmatrix} {}^{t+\Delta t} \mathbf{F}_v^{i-1} \\ {}^{t+\Delta t} \mathbf{F}_p^{i-1} \end{Bmatrix} \quad (17)$$

The left upper index “t+Δt” denotes that the quantities are evaluated at the end of time step, i is the number of iteration. The matrix M_v is mass matrix, K_{vv} and J_{vv} are convective matrices, $K_{\mu v}$ is the viscous matrix, K_{vp} is the pressure matrix, and F_v and F_p are forcing vectors.

Matrix equations will change if penalty formulation is used. For penalty formulation there is a constraint for incompressibility, as it is given in Equation (18):

$$\text{div} \mathbf{v} + \frac{p}{\lambda} = 0 \quad (18)$$

Here in Equation (18) parameter λ is a relatively large positive number (scalar). On that way ratio p / λ becomes a really small number, practically zero.

The incremental-iterative form of the equilibrium equations are

$$\left(\frac{1}{\Delta t} \mathbf{M}_v + {}^{t+\Delta t} \mathbf{K}_{vv}^{i-1} + {}^{t+\Delta t} \mathbf{K}_{\mu v}^{i-1} + {}^{t+\Delta t} \hat{\mathbf{K}}_{\mu v}^{i-1} + {}^{t+\Delta t} \mathbf{J}_{vv}^{i-1} + \mathbf{K}_{\lambda v} \right) \Delta \mathbf{v}^i = {}^{t+\Delta t} \hat{\mathbf{F}}_v^{i-1} \quad (19)$$

Arbitrary Lagrangian Eulerian (ALE) formulation

ALE formulation was employed for fluid domain and mesh moving algorithm for motion of the solid and fluid mesh. ALE formulation are derived and transformed to the FE equations of balance of linear momentum (Donea et al. 1982 [2], Donea 1983 [3], Nitikitpaiboon and Bathe 1993 [9], Filipovic 1999 [4], Filipovic et al. 2006 [5]).

The fluid flow is modeled here using a moving mesh. The reference domain - the FE mesh, in which usual FE calculations are performed, is moving in space. The control volume, which in this case is the volume of a finite element, changes with time. At a point G of the FE mesh Figure 3, the fluid velocity is v and the mesh velocity is v_m . Consequently, in deriving the FE equations for mass balance and balance of linear momentum, the fact that the reference domain is not stationary must be taken into account.

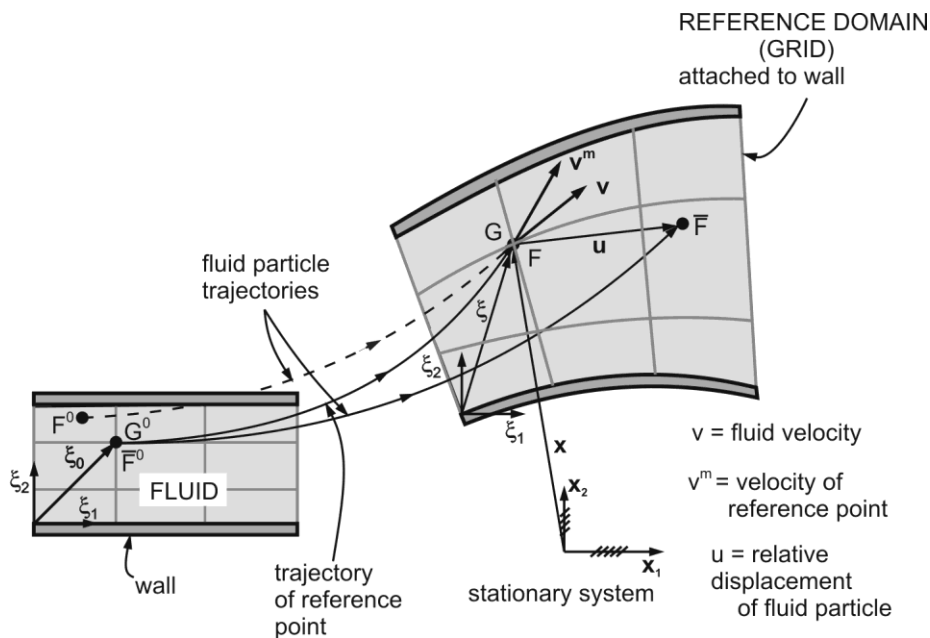


Figure 3: Schematics of the FE modeling according to the ALE formulation (2D representation). A FE mesh attached to the solid is moving in space, changing also its size and shape. The current position of the fluid particle is F and the point of the mesh (grid) is G , with velocities v and v_m ; their initial positions are F^0 and G^0 . Note that the fluid point \bar{F}^0 initially at G^0 is at space position \bar{F} different from F , displaced by a vector u . The coordinate system in the reference domain ξ_1, ξ_2 moves with the reference domain, without rotation.

The Navier – Stokes equations of balance of linear momentum can be written in the ALE formulation (Equation 20).

$$\rho \left[v_i^* + v_j - v_j^m v_{i,j} \right] = -p_{,i} + \mu v_{i,jj} + f_i^V \quad (20)$$

Here v_i are the velocity components of a generic fluid particle and v_i^m are the velocity components of the point on the moving mesh occupied by the fluid particle. The symbol ‘*’ denotes the mesh-referential time derivative, i.e. the time derivative at a considered point on the mesh,

$$\bullet^* = \frac{\partial(\bullet)}{\partial t} \Big|_{\xi_i = \text{const}} \quad (21)$$

The Cartesian spatial coordinates of a generic fluid particle are x_i and of the corresponding point on the mesh are ξ_i . In deriving Equation (20) we used the following expression for the material derivative $D(\rho v_i) / Dt$,

$$\frac{D(\rho v_i)}{Dt} = \frac{\partial(\rho v_i)}{\partial t} \Big|_{\xi} + (v_j - v_j^m) \frac{\partial(\rho v_j)}{\partial x_i} \quad (22)$$

The first term on the right-hand side is the so-called ‘the mesh-referential time derivative’, while the second is the convective term.

The Galerkin method for the space discretization of the fluid domain can now be applied. The finite element equations for a 3D domain are:

$$\begin{aligned} & \rho \int_V N_K v_i^* dV + \rho \int_V N_K v_j - v_j^m v_{i,j} dV = \\ & = - \int_V N_K p_{,i} dV + \int_V \mu N_K v_{i,jj} dV + \int_V N_K f_i^V dV \end{aligned} \quad (23)$$

$$\int_V \bar{N}_k v_{i,i} dV = 0 \quad (24)$$

The integration is performed over the volume V of a finite element, which now is time dependent, using the Gauss theorem.

Consider first the system of Equations (23) which is nonlinear with respect to the velocities, but also with the element volume change. In an incremental analysis a linearization with respect to time must be performed using the known values at the start of time step n . The approximation for a quantity F can be written as:

$${}^{n+1}F \Big|_{n\xi} = {}^nF \Big|_{n\xi} + F^* \Delta t \quad (25)$$

This relation is further applied to the left and right hand sides, (LHS) and (RHS), of Equation (23) to obtain

$${}^n(LHS) + (LHS)^* \Delta t = {}^{n+1}(RHS) \quad (26)$$

In calculating the mesh-referential time derivatives we use the relations:

$$\left(\frac{\partial F}{\partial x_i} \right)^* = \frac{\partial F^*}{\partial x_i} - \left(\frac{\partial v_k^m}{\partial x_i} \right) \frac{\partial F}{\partial x_k} \quad (27)$$

and

$$(dV)^* = \frac{\partial v_k^m}{\partial x_k} dV \quad (28)$$

With these linearizations the Equations (23) and (24) can be written as

$${}^n\mathbf{M}_{(1)} \mathbf{V}^* + {}^n\mathbf{K}_{(1)vv} \Delta \mathbf{V} + {}^n\mathbf{K}_{vp} \Delta \mathbf{P} = {}^{n+1} \mathbf{F}_{(1)} - {}^n \mathbf{F}_{(1)} \quad (29)$$

and

$${}^n\mathbf{M}_{(2)} \mathbf{V}^* + {}^n\mathbf{K}_{(2)vv} \Delta \mathbf{V} = {}^{n+1} \mathbf{F}_{(2)} - {}^n \mathbf{F}_{(2)} \quad (30)$$

The integrals are evaluated over the known FE volumes and surfaces at start of time step. Further, some of the terms are calculated using the values at the last iteration. Of course, the mesh-referential time derivatives V^* and P^* are replaced by $V^* = \Delta V / \Delta t$ and $P^* = \Delta P / \Delta t$ to obtain the incremental algebraic equations.

The presented formulation of the FE modeling is necessary when the fluid boundaries change significantly over the time period used in the analysis. It is particularly convenient when the boundary of the fluid represents a deformable solid, as Figure 3 suggests, for appropriate modeling the solid-fluid interactions. Finally, note that the mesh motion is arbitrary and for each problem can be specifically designed. Also, it is important to emphasize that the solution for the fluid flow does not depend on the FE mesh motion (Filipovic et al. 2006 [5]).

1.4 SOLID – FLUID INTERACTION

Because there are fluid and solid in model and contact between two of them, solid – fluid interaction exists. Assembling of the system of the equations for solid – fluid interaction could be accomplished in two manners: loose coupling and strong coupling. Here, we use loose coupling method.

Loose coupling method

The loose coupling approach consists in the successive solutions for the solid and fluid domains. Consider fluid flow with a deformable solid shown schematically in the Figure 4. The solid deforms due to loading from the fluid which generates surface forces that are transferred to the solid. The stresses acting on the solid surface are the tangential stresses τ_{rad} and τ_{ax} and the normal stress σ_n . The flow domain changes due to the solid deformation, while the common nodes have the same displacements and velocities for the fluid and solid.

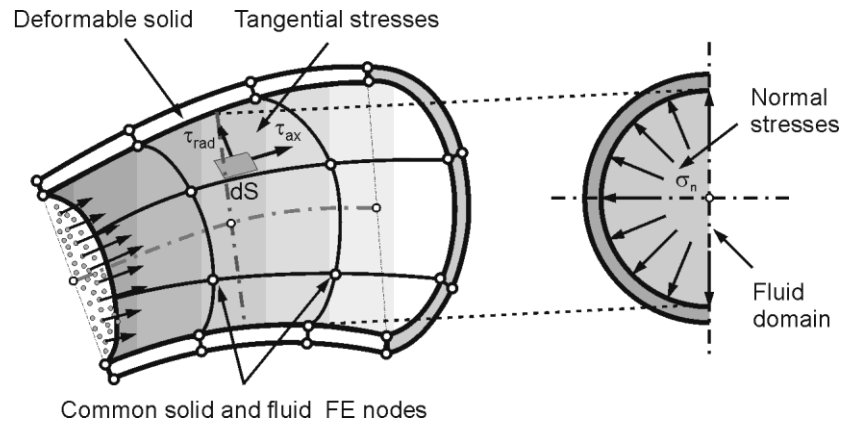


Figure 4: Illustration of the solid-fluid interaction. A fluid is flowing through the deformable solid producing tangential and normal stresses on the solid surface. The common solid and fluid FE nodes have the same displacements and velocities.

The solution is obtained iteratively, and the iteration counter in the solid-fluid interaction loop is ' l '. We have denoted by $^{(n+1)}\sigma_{Sf}^{(l)}$ the stress within the fluid, at the common boundary S . Also, ε_{disp} and $\varepsilon_{velocity}$ are the error tolerances, respectively, for the norms of displacement increments of the solid and for the velocity increments. Other convergence criteria may also be used, such as the error in the 'unbalanced force' or energy (Bathe 1996 [1], Kojic and Bathe 2005 [7]).

For the model we applied following scheme:

1. For the current geometry of the fluid domain determine fluid flow with use of the ALE formulation (Filipovic et al. 2006 [5]). Solid velocities at the common fluid – solid surface are considered as the boundary condition for the fluid.
2. Calculate the loads, arising from the fluid, which act on the solid.
3. Determine deformation of the solid taking the current loads from the fluid domain.
4. Check for the overall convergence which includes fluid and solid. If convergence is reached, go to the next time step. Otherwise go to the next iteration, go to the step 1.

The fluid domain geometry and velocities at the common solid-fluid boundary for the new calculation of the fluid flow are updated (Kojic et al. 2008 [8], Isailovic et al. 2013 [6]). In case of large solid displacements, the FE mesh for the fluid flow domain is updated. Go to step 1.

A graphical interpretation of the algorithm for the solid-fluid interaction problem is shown in Figure 5 (Filipovic 1999 [4]).

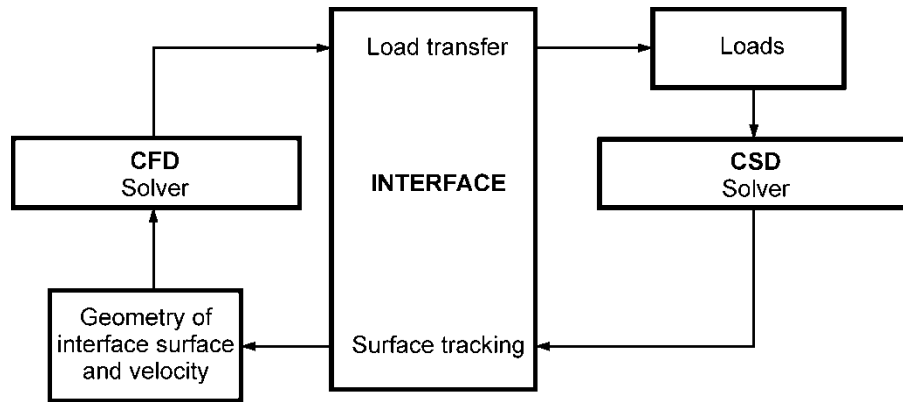


Figure 5:Block-diagram of the solid-fluid interaction algorithm. Information and transfer of parameters between the CSD (computational solid dynamics) and CFD (computational fluid dynamics) solvers through the interface block.

Validation for the loose coupling solid – fluid interaction solver

For validation of the loose coupling solid – fluid interaction solver was used benchmark of viscous flow in a collapsible tube. Fluid flow through collapsible tubes is a complex problem due to the interaction between the tube-wall and the flowing fluid.

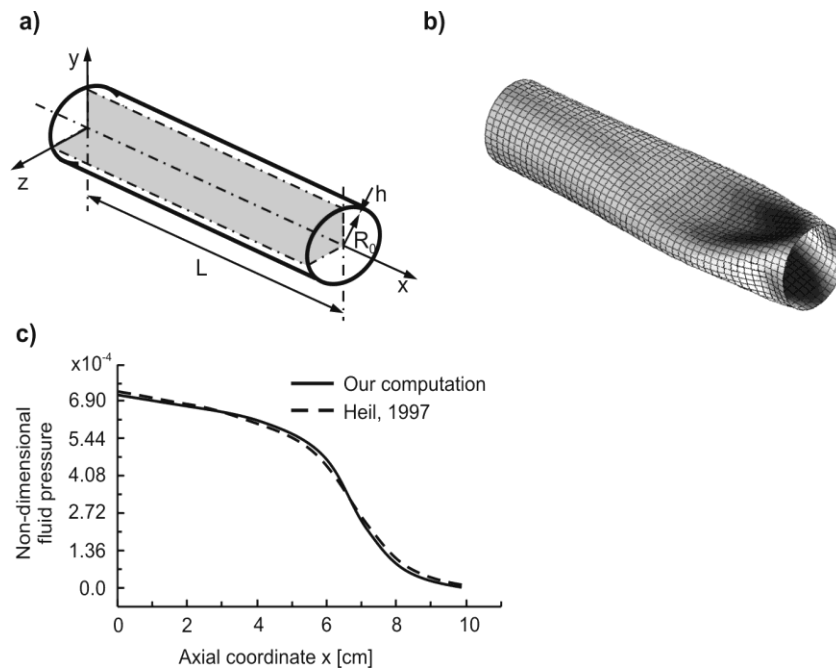


Figure 6: Collapse of a tube loaded by external pressure p_{ext}^* , and with flowing fluid through the tube. **a)** Tube geometry before collapse; **b)** Shape of the tube after collapse; **c)** Pressure distribution along the collapsed tube (at

the tube center line).Data: Lengths [cm] $R_0 = 1, L = 10, h = 0.05$; Non-dimensional volume flux

$$q = 8\mu\dot{V}L / \pi R_0^4 E = 15 \cdot 10^{-5}, \text{ dimensionless external pressure } p_{ext} = p_{ext}^* / E = 6.38 \cdot 10^{-4}.$$

It is assumed that the collapse is symmetric with respect to both x-y and x-z planes. One quarter of the fluid flow field is modeled due to symmetry with respect to the two coordinate planes. Boundary conditions consist of: prescribed velocity at the inlet nodes (zero-velocity at the interface surface with the shell elements) and the symmetry conditions at the symmetry planes. Fluid flow is calculated by using 1250 eight-node 3D elements, and 500 four-node shell elements for the model of the tube wall, with the wall thickness ratio $h/R_0=1/20$ (Filipovic 1999 [5]).

We keep the fluid pressure equal to zero at the tube outer end, and induce the tube collapse by increasing the chamber pressure, p_{ext}^* . The tube is first inflated when $p_{ext}^* = 0$, deforming axisymmetrically. A small geometric irregularity is introduced to initiate the collapse. Then, the external pressure is increased and when it exceeds a critical value, the wall locally loses its stability and the tube buckles as shown in Figure 6b). Figure 6c) shows the pressure drop along on the tube center line.

2 REFERENCES

- [1] Bathe KJ (1996). Finite Element Procedures. Prentice-Hall, Inc., Englewood Cliffs, N.J.
- [2] Donea J, Giuliani S, Halleux JP (1982). An arbitrary Lagrangian-Eulerian finite element method for transient dynamic fluid-structure interactions, *Comp. Meth. Appl. Mech. Engrg.*, 33, 689-723.
- [3] Donea J (1983). Arbitrary Lagrangian-Eulerian finite elements methods. In: Computational Methods for Transient Analysis. edited by Belytschko T, Hughes TJR, 473-516, Elsevier Science Publishers B.V.
- [4] Filipovic N (1999). Numerical Analysis of Coupled Problem: Deformable Body and Fluid Flow. Ph.D. Thesis, Faculty of Mech. Engrg., University of Kragujevac.
- [5] Filipovic N, Mijailovic S, Tsuda A, Kojic M (2006). An Implicit Algorithm within the Arbitrary Lagrangian-Eulerian Formulation for Solving Incompressible Fluid Flow with Large Boundary Motions, *Comp. Meth. Appl. Mech. Engrg.*, 195, 6347-6361.
- [6] Isailovic V., Obradovic M., Nikolic D., Saveljic I. and Filipovic N., SIFEM Project: Finite Element Modeling of the Cochlea, BIBE 2013 - 13th IEEE International Conference on Bioinformatics and BioEngineering, 11-13 November 2013, Chania, Crete, Greece.
- [7] Kojic M, Bathe KJ (2005). Inelastic Analysis of Solids and Structures. Springer-Verlag, Berlin-Heidelberg.
- [8] Kojic M., Filipovic N., Stojanovic B., & Kojic N., "Computer Modeling in Bioengineering – Theoretical Background, Examples and Software". John Wiley and Sons, 978-0-470-06035-3, England, 2008.
- [9] Nitikitpaiboon C, Bathe KJ (1993). An arbitrary Lagrangian-Eulerian velocity potential formulation for fluid-structure interaction, *Computers&Structures*, 47, 871-891.